Applied Surface Science 278 (2013) 207–210

Contents lists available at SciVerse ScienceDirect

Applied Surface Science

journal homepage: www.elsevier.com/locate/apsusc

Functionalized porphyrin conjugate thin films deposited by matrix assisted pulsed laser evaporation

S. Iordache[a], R. Cristescu[b,*], A.C. Popescu[b], C.E. Popescu[b], G. Dorcioman[b], I.N. Mihailescu[b], A.A. Ciucu[c], A. Balan[a], I. Stamatin[a], E. Fagadar-Cosma[d], D.B. Chrisey[e]

[a] University of Bucharest, 3Nano-SAE Research Center, PO Box MG-38, Bucharest-Magurele, Romania
[b] National Institute for Lasers, Plasma & Radiation Physics, Lasers Department, P.O. Box MG-36, Bucharest-Magurele, Romania
[c] University of Bucharest, Faculty of Chemistry, Bucharest, Romania
[d] Institute of Chemistry Timisoara of Romanian Academy, M. Viteazul Ave. 24, 300223-Timisoara, Romania
[e] Tulane University, Departments of Physics & Biomedical Engineering, New Orleans, LA 70118, USA

ARTICLE INFO

Article history:
Received 2 July 2012
Received in revised form 11 January 2013
Accepted 11 January 2013
Available online 18 January 2013

Keywords:
Glucosensor applications
Porphyrin
Thin films
Matrix assisted pulsed laser evaporation

ABSTRACT

We report on the deposition of nanostructured porphyrin-base, 5(4-carboxyphenyl)-10,15,20-tris(4-phenoxyphenyl)-porphyrin thin films by matrix assisted pulsed laser evaporation onto silicon substrates with screen-printed electrodes. AFM investigations have shown that at 400 mJ/cm^2 fluence a topographical transition takes place from the platelet-like stacking porphyrin-based nanostructures in a perpendicular arrangement to a quasi-parallel one both relative to the substrate surface. Raman spectroscopy has shown that the chemical structure of the deposited thin films is preserved for fluences within the range of 200–300 mJ/cm^2. Cyclic voltammograms have demonstrated that the free porphyrin is appropriate as a single mediator for glucose in a specific case of screen-printed electrodes, suggesting potential for designing a new class of biosensors.

1. Introduction

Porphyrins are tetrapyrollic systems whose derivatives are interesting for potential applications in chemistry, biology and medicine. They can be used as photosensitizers for photodynamic therapy [1,2], DNA binding and cleavage [3], and as catalysts for oxydation and reduction chemical reactions [4,5]. However, one of the most prominent applications of porphyrin derivatives is in the sensors field. Porphyrins have been proposed for various types of sensors with signal transduction based on vibration, fluorescence and electrical resistance and/or capacitance. Ref. [6] reviews the use of modified porphyrins with quartz microbalances demonstrating a broad selectivity. Resistive–capacitive sensors based on porphyrin derivatives have been tested and proven functional as temperature, humidity, and illumination sensors [7]. A sensor based on the variation of fluorescent properties of lipophillic porphyrins and metalloporphyrins was efficient in detecting Hg^{2+} in water [8].

When used as the sensing receptor in a sensor, porphyrin is usually deposited as a thin film. The most common techniques used for synthesis of such films are spin coating [9,10], sol–gel [11], Langmuir–Blodget [12] and electropolymerization [13]. Matrix assisted pulsed laser evaporation (MAPLE), a method based on the laser ablation of organic materials from a composite frozen target [14,15] has been used to fabricate metalloporphyrin (Co-, Mn-, and Zn-porphyrin) thin films [16,17]. In this work, we have applied MAPLE method to test availability of free-porphyrin structure, namely 5-(4-carboxyphenyl)-10,15,20-tris(4-phenoxyphenyl)-porphyrin, as thin film on screen-printed electrodes (SPE) as a free enzyme glucose amperometric sensors with a large range of detection.

2. Experimental

2.1. Materials

In this work, we used a mixed substituted A_3B porphyrin, namely 5-(4-carboxyphenyl)-10,15,20-tris(4-phenoxyphenyl)-porphyrin (CPPOPP) (Fig. 1). It was obtained based on previously reported methods [18,19] by condensing a mixture of pyrrole and two appropriately substituted benzaldehyde, 4-carboxylmethylbenzaldehyde and 4-phenoxybenzaldehyde, in a particular ratio of 1/3. The methyl ester was hydrolyzed in basic condition folowed by neutralization with diluted HCl. [20]

* Corresponding author. Tel.: +40 21 4574491; fax: +40 21 4574243.
E-mail addresses: rodica.cristescu@inflpr.ro, rocris8991p@yahoo.com (R. Cristescu).

0169-4332/$ – see front matter © 2013 Elsevier B.V. All rights reserved.
http://dx.doi.org/10.1016/j.apsusc.2013.01.080

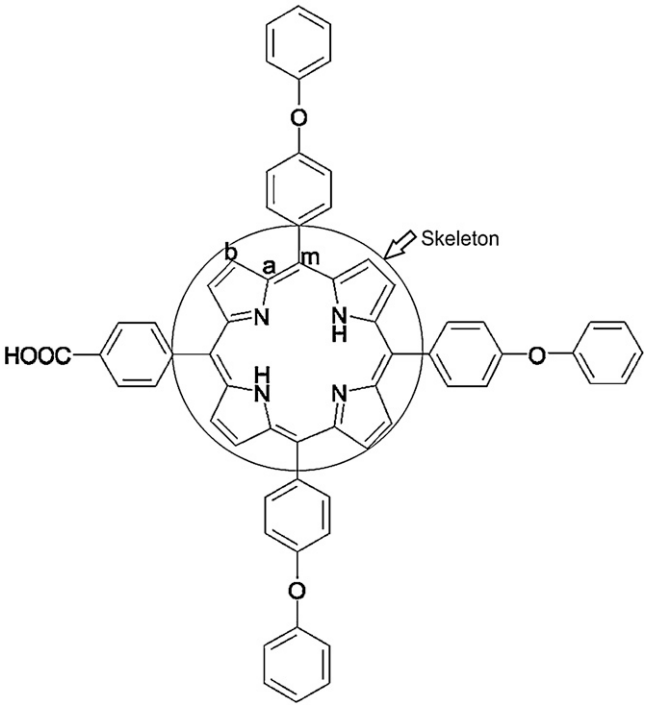

Fig. 1. Chemical structure of 5-(4-carboxyphenyl)-10,15,20-tris(4-phenoxyphenyl)-porphyrin (CPPOPP).

Solutions consisting of 1% CPPOPP in chloroform were prepared and tested. All target solutions were poured into a pre-cooled target holder at 173 K and subsequently immersed in liquid nitrogen for 30 min.

Electrolyte support for cyclic voltammetry was phosphate buffer solution (PBS) with pH 7.4. The screen printed electrodes used were based on carbon paste (SPE-110, model DropSense 110) consisting of three electrodes in a planar geometry: (1) a working electrode (WE) that consists of a central carbon paste disc with 0.125 cm^2 area; (2) an auxiliary carbon paste ring electrode (counter) placed at 1 mm distance from WE; and (3) an Ag ring pseudoreference electrode. The solution composition ranged from 0.5 mM to 8 mM glucose in PBS. The glucose concentration used in our experiments has covered the range from hypoglycemia (<4 mM) to hyperglycemia (>7 mM).

2.2. MAPLE experiment

Thin films were fabricated by MAPLE and drop-casting. All MAPLE depositions were conducted using a KrF* (λ = 248 nm, τ_{FWHM} = 25 ns, pulse repetition rate = 10 Hz) laser which was operated at a fluence within the range 200–500 mJ/cm^2, and for 10,000–20,000 pulses. The laser spot area was set at 10 mm^2. The target was rotated at a rate of 0.4 Hz during deposition and the laser beam scanned the entire target surface at an angle of 45°. All MAPLE experiments have been conducted at a base pressure of 30–40 Pa. The substrate-to-target distance was 4 cm. The target was maintained at a temperature of ~173 K by active liquid nitrogen cooling. The thin films were deposited onto one-side polished Si(1 0 0) wafers for Raman and AFM measurements, and carbon paste screen-printed electrodes for cyclic voltammetry. All substrates were ultrasonically cleaned prior to deposition by immersion in ethanol, and then dried in air under UV exposure from a VL-115UV lamp.

2.3. Thin films characterization

CPPOPP-porphyrin thin films were characterized by Raman spectroscopy, AFM and cyclic voltammetry. Raman spectra were recorded by Jasco NRS 3100 apparatus with dual laser beams, 532 and 785 nm, respectively. AFM micrographs were registered by Integrated Platform SPM-NTegra model Prima in semi-contact mode, error mode and phase contrast. Cyclic voltammetry tests were performed with a Voltalb 40 system (Radiometer Analytical) adapted for screen-printed electrodes (SPEs). Both electro-oxidation and reduction potentials have been recorded within the range (−500–500) mV with 100 mV/s scan rate. Normal working conditions of temperature and pressure (25 °C and 1 atm) were kept during all experiments.

3. Results and discussion

3.1. AFM investigations

Typical AFM micrographs of CPPOPP thin films obtained by MAPLE at the laser beam fluence of 200 mJ/cm^2 (a), 300 mJ/cm^2 (b), 400 mJ/cm^2 (c), and 500 mJ/cm^2 (d) are given in Fig. 2. Each inset describes morphological type in detail by edge detection with ImageJ program [21]. At small fluences (200 and 300 mJ/cm^2, insets of Figs. 2a and b), the surface mainly consists of small droplets in platelet-like stacking porphyrin-based nanostructures in perpendicular arrangement onto the substrate surface. At higher fluence

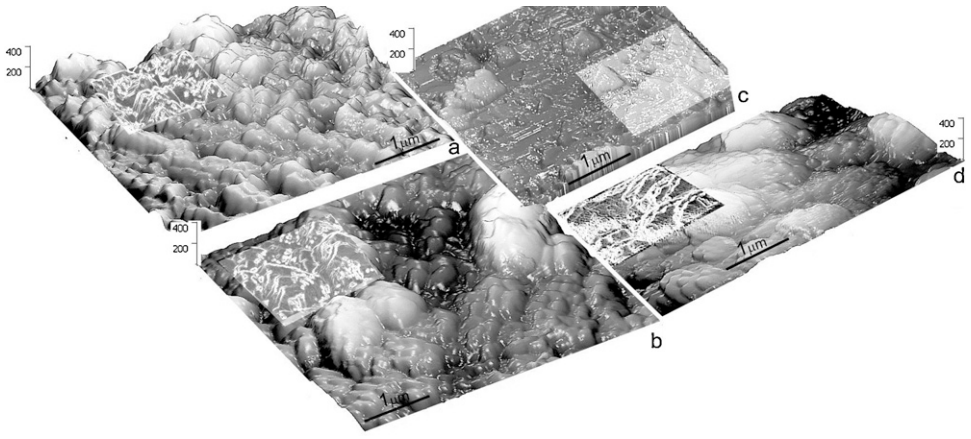

Fig. 2. Typical AFM micrographs of CPPOPP MAPLE-deposited thin films at 200 mJ/cm^2 (a), 300 mJ/cm^2 (b), 400 mJ/cm^2 (c), and 500 mJ/cm^2 (d). The height of AFM profiles is given in nanometers.

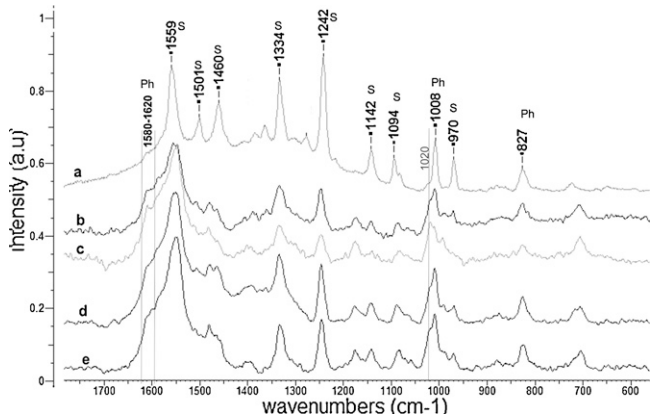

Fig. 3. Typical Raman spectra of CPPOPP dropcast (a) and MAPLE-deposited CPPOPP thin films at 200 mJ/cm^2 (b), 300 mJ/cm^2 (c), 400 mJ/cm^2 (d), and 500 mJ/cm^2 (e). S = Skeleton, Ph = Phenyl side groups (from Fig. 1).

of 400 mJ/cm^2 (inset of Fig. 2c), the porphyrin becomes randomly distributed with platelet-like stacking that is not well-defined. At fluence of 500 mJ/cm^2, the platelet-like stacking surface structures seem re-arranged in a quasi-parallel related to the substrate surface (see inset of Fig. 2d). It appears that at 400 mJ/cm^2 fluence a topographical transition takes place from the platelet-like stacking porphyrin-based nanostructures in a perpendicular arrangement to a quasi-parallel one both relative to the substrate surface.

From Fig. 2, we inferred that the thickness has reached 200 nm for 200 mJ/cm^2 fluence and 400 nm for 300 mJ/cm^2 laser fluence, respectively (both cases corresponding to perpendicular orientation). For thin films deposited at 400 mJ/cm^2 laser fluence the thickness was 400 nm, while for 500 mJ/cm^2 fluence the thickness was 800 nm.

3.2. Raman spectroscopy

Raman spectra of CPPOPP compound drop-cast (a) and MAPLE-deposited thin films at 200 mJ/cm^2 (b), 300 mJ/cm^2 (c), 400 mJ/cm^2 (d), and 500 mJ/cm^2 (e), are shown in Fig. 3. The typical group fingerprints Raman bands between 1000 and 1600 cm^{-1} consistent with CPPOPP complex structure are assigned to porphyrin skeleton and phenyl groups. Both Raman spectral bands data and corresponding assignments are summarized in Table 1. These data are in accordance with those given in Ref [22]. The porphyrin skeleton bands (symbol "S" in Fig. 3) exhibit small shifts in wavelength in comparison with the dropcast ones. There is a slight difference in terms of broadening between dropcast and MAPLE-deposited film bands. The aforementioned topographical transition is accompanied by: (i) increase the phenyl band intensity at 1580–1620 cm^{-1}; (ii) significant decrease of skeleton band intensity with lower fluence (200 and 300 mJ/cm^2) followed by an increase with higher fluences (400 and 500 mJ/cm^2) at 1501 and 1460 cm^{-1}; (iii) development of 1020 cm^{-1} band with fluence; and (iv) vanishing of 970 cm^{-1} band intensity with fluence.

Table 1
Band assignments in Raman spectra of CPPOPP [22].

Band (cm^{-1})	Assigned band	Group
1580–1620	Phenyl	Phenyl rings
1559	ν(C$_a$–C$_m$) asymm	Porphyrin ring-skeleton
1501	ν(C$_b$–C$_b$)	Pyrrole-skeleton
1460	ν(C$_a$–C$_m$) sym	Porphyrin ring
1334	ν(pyr quarter-ring), ν(pyr half-ring) sym	Pyrrole-skeleton
1242	δ(C$_b$–H) asym	Pyrrole-skeleton
1142	N–H bend ν(C$_a$–N) asym	Pyrrole-skeleton
1094	δ(C$_b$–H) sym	Pyrrole-skeleton
1020	ν(pyr breath)	Skeleton
1008	Phenyl + ν(pyr half-ring) asym, ν(pyr breath)	Phenyl + skeleton
970	ν(pyr half-ring) asym + phenyl	Skeleton
827	δ(pyr def) asym	Pyrrole-skeleton

ν – stretching, δ – deformation.

Due to the fact that the perpendicular stacking of the porphyrinic skeleton is more appropriate in order to expose the functional groups (phenyl and carboxyl, see Fig. 1), the optimum fluence value was set at 300 mJ/cm^2. In addition, the phenyl group is inert to the analytes (e.g., glucose) and, thus, the only available reactive groups remain external COOH group or the two internal NH groups that work as proton donors. In this respect, the porphyrin works as only one-way electron–proton transfer in a redox reaction (in our case, hydrogen atom transfer). In order to investigate this assumption, the cyclic voltametry was applied on the MAPLE-deposited CPPOPP films for 300 mJ/cm^2 fluence.

3.3. Cyclic voltammetry

Cyclic voltammetry is useful for rapid identification of analytes from blood samples and diagnostic of interaction analyte–substrate and oxidation–reduction reaction occurring with electron transfer [23]. A simple current–voltage scan at a given scan rate in a three electrode-micro-electrochemical cell such as SPE allows for simple tests that identify both the oxidation–reduction potential and the current density. The underlying principle to design the prototype of a biosensor consists of checking the substrate capability as a good mediator for an appropriate reaction. The most investigated biosensor relies on the rapid blood glucose measurements based on glucose-oxidase and different mediators such as ferrocene [24] or dye such as Prussian blue [25], and semiconducting polymers [26]. The glucose oxidase is unstable and need protection against environment condition, also mediators induce deterioration in amperometric sensors based on glucose-oxidase electrode. The research is currently oriented to simple mediator and substrate with redox properties.

Porphyrin can convert glucose to gluconolactone during the oxidation reaction performed in a buffer solution. The electrochemical response of MAPLE-deposited CPPOPP-porphyrin thin films on SPE to glucose is shown in (Fig. 4).

Cyclic voltamogramms (Fig. 4a) indicate a specific electrochemical activity in PBS with an oxidation potential at 30 mV shifting the equilibrium to acidic pH (otherwise not observed in other reports with different mediators and glucose-oxidase [24,25]). This proves that the porphyrin has an electrochemical activity related to glucose oxidation. For PBS-glucose solutions the oxidation potential shifts to 50–60 mV (slightly dependent on concentration) and peak current density has a quasi-linear dependence vs. concentration (Fig. 4b). It is known that the electro-oxidation and reduction states are well defined in acidic media [27]. Usually, perchloric acid (as proton donor for acylation of glucose) is added in buffer solution [28]. In the presence of the proton donor (the perchloric acid), the glucose converts to various forms of gluconate radicals with a specific electrochemical response.

In our case, the proton donor is mediated also by porphyrins in a secondary reaction of oxidation of the water in the buffer solution as seen in Fig. 4a (PBS curve). In general, the biosensors based on glucose-oxidase-mediators in buffer solutions with perchloric acid as support electrolyte have the oxidation potential ~300 mV vs. standard calomel electrode (SCE). In this work, the electro-oxidation potential ranges at 50–60 mV vs. pseudo reference electrode. Therefore, the porphyrins decrease the high activation energy to mediate an electro-oxidation reaction due to the high capacity to donate protons. In Fig. 4b, the peak of

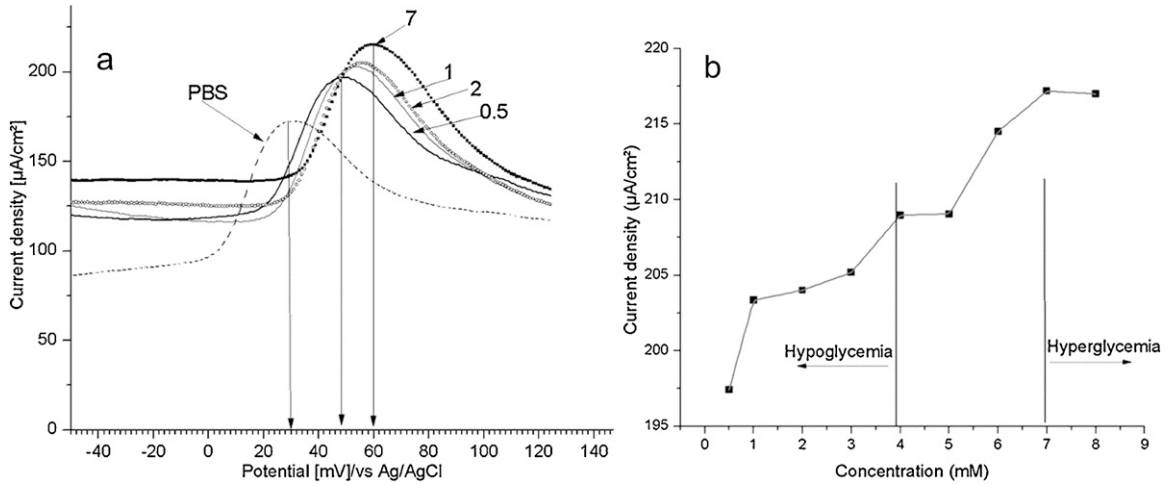

Fig. 4. Typical cyclic voltammograms of MAPLE-deposited CPPOPP thin films on SPE-110 at 300 mJ/cm^2 laser fluence in case of 0.5 mM, 1 mM, 3 mM, and 7 mM glucose concentrations in PBS: (a) Current density vs. potential for PBS and PBS and glucose vs. Ag-pseudoreference electrode (equivalent with Ag/AgCl), and (b) Peak current density vs. concentration in the range 0.5–8 mM glucose concentration.

current densities recorded vs. concentration has a large response for glucose covering hypo- and hyper-glycemic area.

4. Conclusions

We have demonstrated that MAPLE technique is suitable for the immobilization of functionalized porphyrin, CPPOPP thin films. AFM investigations have shown that thin films have a quasi-continuous morphology dependent on incident laser fluence. Raman spectroscopy investigations have confirmed that the chemical structure of MAPLE-deposited thin films is preserved for laser fluence values of 200–300 mJ/cm^2. Cyclic voltammograms have demonstrated that the free porphyrin is appropriate as a single mediator for glucose in the specific case of carbon paste screen-printed electrodes, suggesting free enzymatic biosensors design using porphyrins only.

Acknowledgments

This work was supported by the grants of the Romanian National Authority for Scientific Research, CNCS-UEFISCDI, project numbers PN-II-ID-PCE-2011-3-0888 (209/5.10.2011) and PN-II-ID-PCE-2011-3-0815 (64/5.10.2011).

References

[1] A. Wiehe, Y.M. Shake, J.C. Brandt, S. Mebs, M.O. Senge, Tetrahedron 61 (23) (2005) 5535–5564.
[2] H.M. Wang, J.Q. Jiang, J.H. Xiao, R.L. Gao, F.Y. Lin, X.Y. Liu, Chemico-Biological Interactions 172 (2) (2008) 154–158.
[3] P. Zhao, L.C. Xu, J.W. Huang, K.C. Zheng, B. Fu, H.C. Yu, L.N. Ji, Biophysical Chemistry 135 (1–3) (2008) 102–109.
[4] A. Rezaeifard, M. Jafarpour, A. Naeimi, Catalysis Communications 16 (1) (2011) 240–244.
[5] S.N.S. Goubert-Renaudin, X. Zhu, A. Wieckowski, Electrochemistry Communications 12 (11) (2010) 1457–1461.
[6] C. Di Natale, R. Paolesse, A. Macagnano, A. Mantini, P. Mari, A. D'Amico, Sensors and Actuators B: Chemical 68 (1–3) (2000) 319–323.
[7] M. Saleem, M.H. Sayyad, K.S. Karimov, M. Yaseen, M. Ali, Sensors and Actuators B: Chemical 137 (2) (2009) 442–446.
[8] Y. Yang, J. Jiang, G. Shen, R. Yu, Analytica Chimica Acta 636 (1) (2009) 83–88.
[9] J. Spadavecchia, G. Ciccarella, P. Siciliano, S. Capone, R. Rella, Sensors and Actuators B: Chemical 100 (1–2) (2004) 88–93.
[10] B. Wang, X. Zuo, Y. Wu, Z. Chen, C. He, W. Duan, Sensors and Actuators B: Chemical 152 (2) (2011) 191–195.
[11] S. Nardis, D. Monti, C. Di Natale, A. D'Amico, P. Siciliano, A. Forleo, M. Epifani, A. Taurino, R. Rella, R. Paolesse, Sensors and Actuators B: Chemical 103 (1–2) (2004) 339–343.
[12] D. Çaycı, S.G. Stanciu, İ. Çapan, M. Erdoğan, B. Güner, R. Hristu, G.A. Stanciu, Sensors and Actuators B: Chemical 158 (1) (2011) 62–68.
[13] R. Paolesse, C. Di Natale, V. Campo Dall'Orto, A. Macagnano, A. Angelaccio, N. Motta, A. Sgarlata, J. Hurst, I. Rezzano, M. Mascini, A. D'Amico, Thin Solid Films 354 (1–2) (1999) 245–250.
[14] R.A. McGill, D.B. Chrisey, Patent number 6,025,036 (2000).
[15] D.B. Chrisey, R.A. McGill, J.S. Horwitz, A. Pique, B.R. Ringeisen, D.M. Bubb, P.K. Wu, Chemical Reviews 103 (2003) 553–576.
[16] R. Cristescu, C. Popescu, A.C. Popescu, I.N. Mihailescu, A.A. Ciucu, A. Andronie, S. Iordache, I. Stamatin, E. Fagadar-Cosma, D.B. Chrisey, Materials Science and Engineering B-Advanced Functional Solid-State Materials 169 (1–3) (2010) 106–110.
[17] R. Cristescu, C. Popescu, A.C. Popescu, S. Grigorescu, I.N. Mihailescu, A.A. Ciucu, S. Iordache, A. Andronie, I. Stamatin, E. Fagadar-Cosma, D.B. Chrisey, Applied Surface Science 257 (12) (2011) 5293–5297.
[18] D. Vlascici, E. Fagadar-Cosma, I. Popa, V. Chiriac, M. Gyl-Agusti, Sensors 12 (2012) 8193–8203.
[19] E. Fagadar-Cosma, G. Fagadar-Cosma, M. Vasile, C. Enache, Current Organic Chemistry 16 (2012) 931–941.
[20] E. Fagadar-Cosma, L. Cseh, V. Badea, G. Fagadar-Cosma, D. Vlascici, Combinatorial Chemistry & High Throughput Screening 10 (2007) 466–472.
[21] R. Syed, N. Sobh, U. Ravaioli, G. Popescu, M. Mohamed, imageJ (2012), http://dx.doi.org/10.4231/D3DR2P78G http://nanohub.org/resources/imagej
[22] D. Wang, X. Cheng, Y. Shi, E. Sun, X. Tang, C. Zhuang, T. Shi, Solid State Sciences 11 (2009) 195–199.
[23] D. Grieshaber, R. MacKenzie, J. Vörös, E. Reimhult, Sensors 8 (2008) 1400–1458.
[24] A.E.G. Cass, G. Davis, G.D. Francis, H.A.O. Hill, W.J. Aston, I. John Higgins, E.V. Plotkin, L.D.L. Scott, A.P.F. Turner, Analytical Chemistry 56 (1984) 667–671.
[25] F. Ricci, A. Amine, C.S. Tuta, A.A. Ciucu, F. Lucarelli, G. Palleschi, D. Moscone, Analytica Chimica Acta 485 (1) (2003) 111–120.
[26] D. Bélanger, J. Nadreau, G. Fortier, Journal of Electroanalytical Chemistry and Interfacial Electrochemistry 274 (1–2) (1989) 143–155.
[27] X. Wang, M. Lu, C. Huo, H. Li, Y. Wang, Z. Li, Spectrochimica Acta, Part A 73 (2009) 581–586.
[28] B. Mukhopadhyay, D.A. Russell, R.A. Field, Carbohydrate Research 340 (2005) 1075–1080.